Available online at www.sciencedirect.com
ScienceDirect
Journal of the European Ceramic Society 29 (2009) 2423–2427
www.elsevier.com/locate/jeurceramsoc

Technical note

# Hot corrosion behavior of $V_2O_5$-coated $Gd_2Zr_2O_7$ ceramic in air at 700–850 °C

Zhan-Guo Liu, Jia-Hu Ouyang *, Yu Zhou, Xiao-Liang Xia

*Institute for Advanced Ceramics, Department of Materials Science, Harbin Institute of Technology, Harbin 150001, China*

Received 30 November 2008; received in revised form 24 December 2008; accepted 8 January 2009
Available online 3 February 2009

**Abstract**

$Gd_2Zr_2O_7$ ceramic was prepared by solid state reaction at 1650 °C for 10 h in air, and exhibited a defect fluorite-type structure. Reaction between molten $V_2O_5$ and $Gd_2Zr_2O_7$ ceramic was investigated at temperatures ranging from 700 to 850 °C using an X-ray diffractometer (XRD) and scanning electron microscopy (SEM). Molten $V_2O_5$ reacted with $Gd_2Zr_2O_7$ to form $ZrV_2O_7$ and $GdVO_4$ at 700 °C; however, in a temperature range of 750–850 °C, molten $V_2O_5$ reacted with $Gd_2Zr_2O_7$ to form $GdVO_4$ and m-$ZrO_2$. Two different reactions observed at 700 °C and 750–850 °C could be explained based on the thermal instability of $ZrV_2O_7$.
© 2009 Elsevier Ltd. All rights reserved.

*Keywords:* $Gd_2Zr_2O_7$; Corrosion; $V_2O_5$

## 1. Introduction

Thermal barrier coatings (TBCs) are widely used to provide thermal insulation for metallic components against the hot gas stream in gas-turbine engines, and to meet the rapidly increasing demands for higher fuel efficiency and greater thrust.[1,2] Up to now, the most successful TBC materials are 6–8 wt.% yttria-stabilized zirconia (YSZ), which are applied on engine hot-section components by plasma spraying or electron beam physical vapor deposition.[3] However, 6–8 wt.%YSZ is limited to applications below 1200 °C.[4] Above 1200 °C, the $t'$-phase zirconia in TBCs transforms into cubic and tetragonal phases. During cooling the tetragonal phase will further transform into the monoclinic phase, which is accompanied with a volume change of 3–5% and a severe damage of TBCs.[5,6]

In recent years, there has been an increasing demand for developing TBC materials with low thermal conductivity and high phase stability. Among high-melting ceramic materials, rare-earth zirconates have a distinctly lower thermal conductivity than 6–8 wt.%YSZ. It was reported that the thermal conductivities of rare-earth zirconate ceramics varied from 1.1 to 2.0 $W\,m^{-1}\,K^{-1}$ from room temperature to 1400 °C.[7–11] In addition, the phase transition temperature of rare-earth zirconates is higher than that of 6–8 wt.%YSZ, such as 2300 °C for $Nd_2Zr_2O_7$, 2000 °C for $Sm_2Zr_2O_7$ and 1530 °C for $Gd_2Zr_2O_7$, respectively.[12] Therefore, rare-earth zirconate ceramics are potential candidates for high-temperature thermal barrier coatings applications. When TBCs are operated with low-quality fuels containing appreciable levels of vanadium, sodium, sulfur, etc., the hot corrosion of 6–8 wt.%YSZ becomes significant.[13] There has been a substantial amount of research reported in

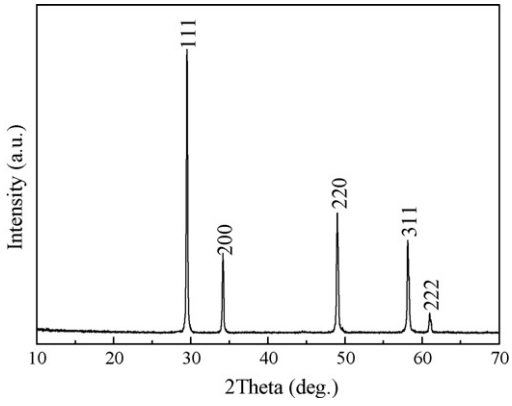


Fig. 1. X-ray diffraction pattern of $Gd_2Zr_2O_7$ ceramic sintered at 1650 °C for 10 h.

* Corresponding author. Tel.: +86 451 86414291; fax: +86 451 86414291.
*E-mail address:* ouyangjh@hit.edu.cn (J.-H. Ouyang).

0955-2219/$ – see front matter © 2009 Elsevier Ltd. All rights reserved.
doi:10.1016/j.jeurceramsoc.2009.01.001

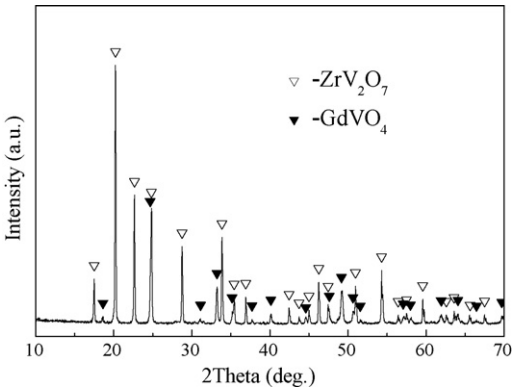


Fig. 2. X-ray diffraction pattern of $V_2O_5$-coated $Gd_2Zr_2O_7$ specimen heat-treated at 700 °C for 2 h.

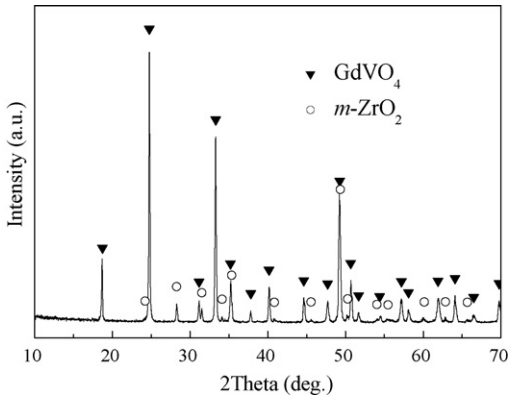


Fig. 4. X-ray diffraction pattern of $V_2O_5$-coated $Gd_2Zr_2O_7$ specimen heat-treated at 750 °C for 2 h.

the literature on the hot corrosion of 6–8 wt.%YSZ coatings by the presence of $V_2O_5$.[14–17] Marple et al. reported that lanthanum zirconate coatings prepared by plasma spraying were relatively resistant to attack by $V_2O_5$ at 1000 °C.[18] These coatings remained well bonded to the substrate following a high-temperature exposure to $V_2O_5$, contained only minor amounts of $LaVO_4$, and exhibited a microstructure little changed from the as-sprayed state. It was reported that $Gd_2Zr_2O_7$ had the lowest thermal conductivity of unary rare-earth zirconates.[9] In the present study, in order to investigate the hot corrosion behavior of $Gd_2Zr_2O_7$ ceramic by molten $V_2O_5$, hot corrosion experiments were performed in a temperature range of 700–850 °C for 2 h in air.

## 2. Experimental procedure

In the present study, $Gd_2Zr_2O_7$ was synthesized by a solid state reaction process. The starting materials were gadolinia (Grirem Advanced Materials Co., Ltd., China; purity ≥99.9%) and zirconia powders (Shenzhen Nanbo Structure Ceramics Co., Ltd., China; purity ≥99.9%) with average particle sizes less than

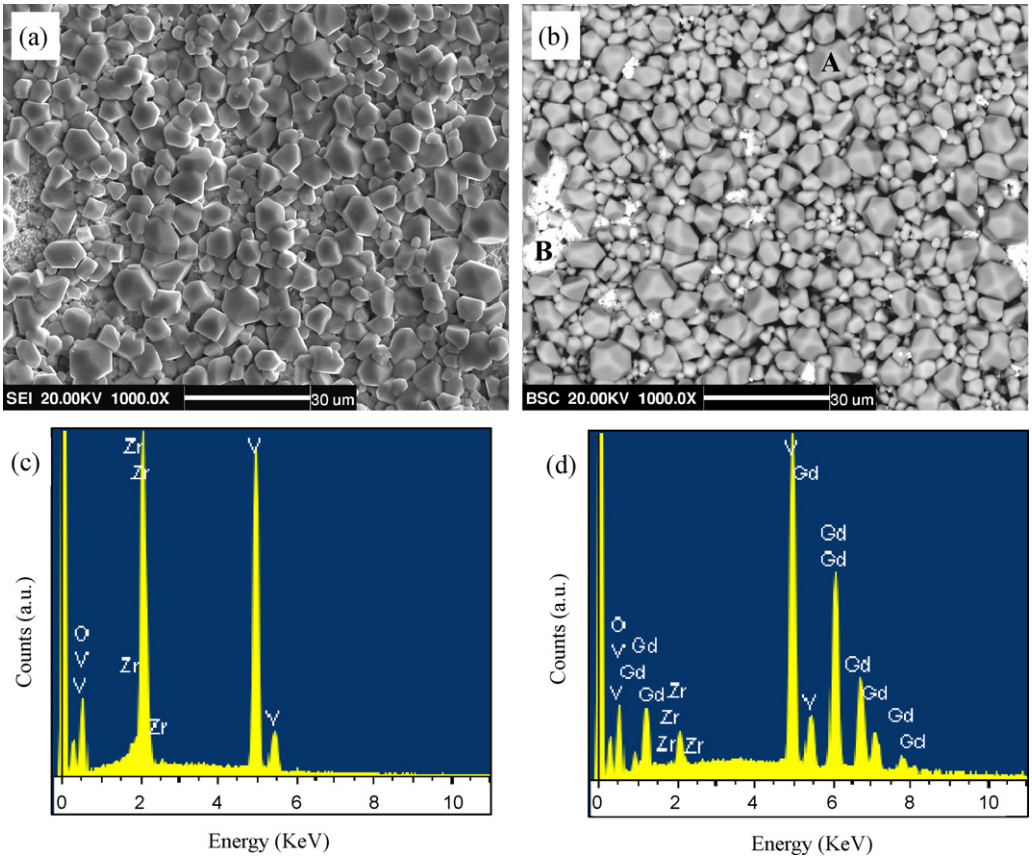


Fig. 3. Microstructures of $V_2O_5$-coated $Gd_2Zr_2O_7$ specimen heat-treated at 700 °C for 2 h: (a) secondary electron micrograph; (b) corresponding backscattered electron micrograph of (a); (c and d) EDS spectra at the locations of A and B, respectively, in (b).

1 μm. Zirconia and gadolinia powders in appropriate ratios were mechanically mixed in analytically pure alcohol for 24 h. The dried powder mixtures were molded by the uniaxial stress. Subsequently, the molded samples were further compacted by the cold isostatic pressing method with a pressure of 280 MPa for 5 min. The compacts were then pressureless-sintered at 1650 °C for 10 h at a heating rate of 300 °C $h^{-1}$ in air.

The specimens with dimensions of 10 mm × 10 mm × 2 mm were machined from the sintered $Gd_2Zr_2O_7$. The specimens were ground to 1500 grit finish, ultrasonically degreased in acetone, and dried at 100 °C over night. The $V_2O_5$ powder was spread uniformly over the $Gd_2Zr_2O_7$ specimen surface at a concentration of 15 mg $cm^{-2}$ using a very fine glass rod that was ultrasonically cleaned and dried. The $V_2O_5$-coated $Gd_2Zr_2O_7$ specimens were then placed in a zirconia crucible which was subsequently covered with a thin zirconia sheet during heat-treatment. The $V_2O_5$-coated $Gd_2Zr_2O_7$ specimens were isothermally heat-treated at different temperature levels ranging from 700 to 850 °C for 2 h in air.

Crystal structures of $Gd_2Zr_2O_7$ and hot corrosion specimens were identified by an X-ray diffractometer (XRD, D/Max-2200VPC, Rigaku Co., Ltd., Japan) with Cu Kα radiation at a scan rate of 3°/min. The microstructural analysis of $Gd_2Zr_2O_7$ and hot corrosion specimens was carried out with a scanning electron microscope (SEM, CamScan MX 2600FE, UK) equipped with energy-dispersive X-ray spectroscopy (EDS,

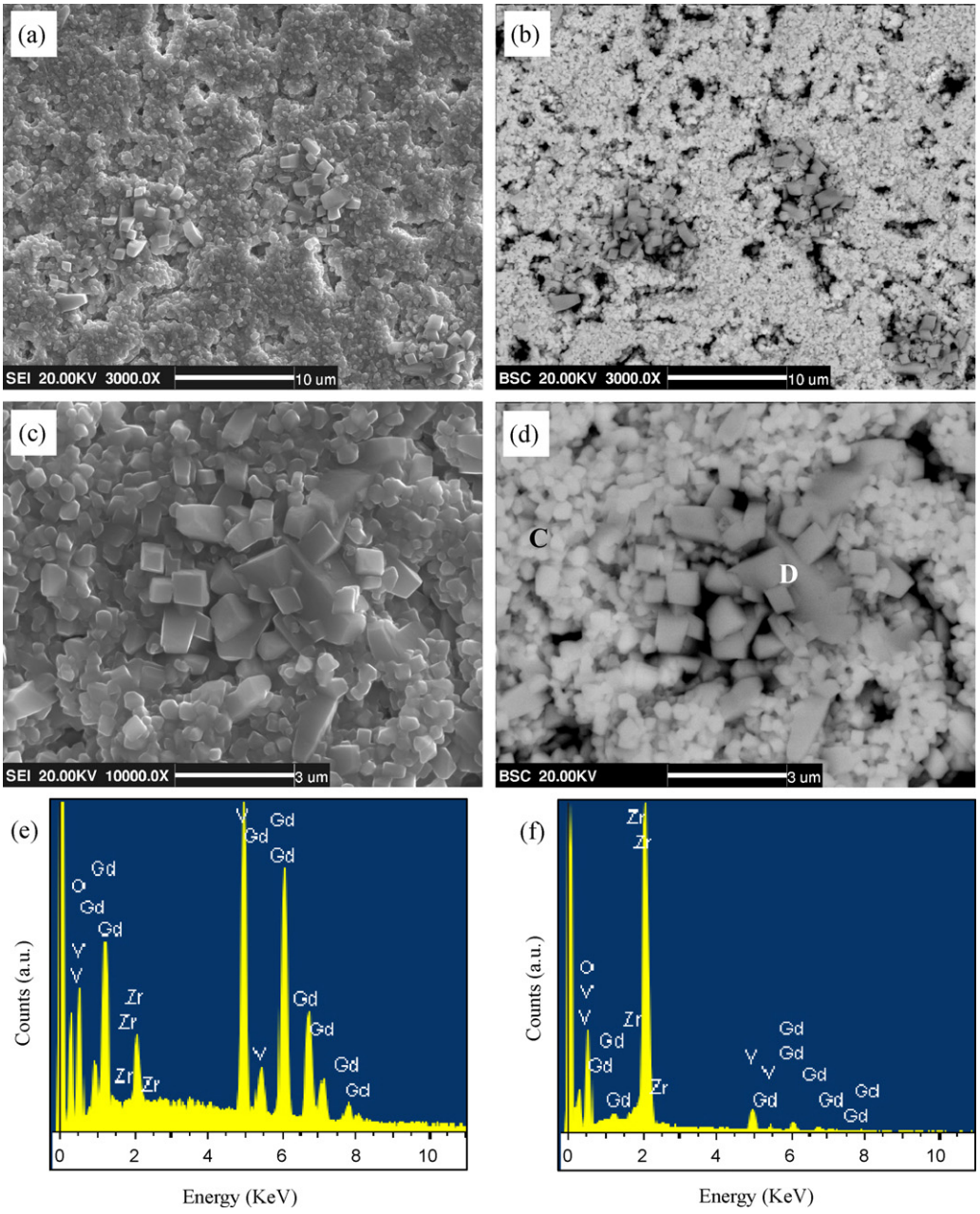


Fig. 5. Microstructures of $V_2O_5$-coated $Gd_2Zr_2O_7$ specimen heat-treated at 750 °C for 2 h: (a and c) secondary electron micrographs; (b and d) corresponding backscattered electron micrographs of (a) and (c), respectively; (e and f) EDS spectra at the locations of C and D, respectively, in (d).

Oxford Instruments INCA X-sight system, 7537, UK) operating at 20 kV. A thin carbon coating was evaporated onto the surface of the specimens for electrical conductivity.

## 3. Results and discussion

Fig. 1 reveals X-ray diffraction pattern of $Gd_2Zr_2O_7$ ceramic sintered at 1650 °C for 10 h in air. It can be seen that $Gd_2Zr_2O_7$ has a single phase of defect fluorite-type structure. It is well known that $Gd_2Zr_2O_7$ undergoes a structural transition from an ordered pyrochlore to a defect fluorite when heated to above 1530 °C.[12] As the sintered temperature (1650 °C) in this work is higher than the order–disorder transition temperature, it is not surprising that $Gd_2Zr_2O_7$ exhibits a defect fluorite-type structure.

During practical high-temperature combustion, vanadium in low-quality fuels reacts with oxygen to form $V_2O_5$. The melting point of $V_2O_5$ is 690 °C. In this study, hot corrosion studies were carried out in the temperature range of 700–850 °C. Fig. 2 shows XRD pattern obtained from the $V_2O_5$-coated $Gd_2Zr_2O_7$ specimen heat-treated at 700 °C for 2 h in air. The newly evolved peaks are due to two different reaction products, zirconium vanadate ($ZrV_2O_7$, JCPDS no. 16–0422) and gadolinium vanadate ($GdVO_4$, JCPDS no. 17–0260). No significant $Gd_2Zr_2O_7$ phase was observed from the XRD analysis. Typical surface morphology of the $V_2O_5$-coated $Gd_2Zr_2O_7$ specimen heat-treated at 700 °C for 2 h is shown in Fig. 3(a) and (b). The EDS spectra obtained at different regions of A and B in Fig. 3(b) confirmed the presence of elements consistent with the formation of reaction products of $ZrV_2O_7$ (region A) and $GdVO_4$ (region B) as shown in Fig. 3(c) and (d). This supports the above XRD results.

The XRD pattern obtained from the $V_2O_5$-coated $Gd_2Zr_2O_7$ specimen heat-treated at 750 °C for 2 h in air is shown in Fig. 4. It can be seen that the diffraction pattern is obviously different from that obtained at 700 °C. No $ZrV_2O_7$ phase is identified at this temperature from the XRD analysis. Besides $GdVO_4$, monoclinic zirconia (m-$ZrO_2$, JCPDS no. 37–1484) is found to exist after chemical reaction at 750 °C for 2 h. Fig. 5 shows the microstructure of the $V_2O_5$-coated $Gd_2Zr_2O_7$ specimen heat-treated at 750 °C for 2 h. From the EDS results in Fig. 5(e) and (f) obtained at different regions in Fig. 5(d), the elements identified are consistent with the presence of reaction products of $GdVO_4$ (region C) and m-$ZrO_2$ (region D) at 750 °C for 2 h. The phase constituents of the $V_2O_5$-coated $Gd_2Zr_2O_7$ specimens heat-treated at 800 or 850 °C for 2 h are consistent with the result obtained at 750 °C for 2 h. Typical microstructures of $V_2O_5$-coated $Gd_2Zr_2O_7$ specimens heat-treated at 800 or 850 °C for 2 h are shown in Fig. 6. From Fig. 6, the microstructure after heat-treatments at 800 or 850 °C for 2 h is very similar to those obtained at 750 °C for 2 h.

Two different chemical reactions are observed at 700 °C and 750–850 °C between $V_2O_5$ and $Gd_2Zr_2O_7$ in this study. This could be explained based on the thermal instability of $ZrV_2O_7$. At 700 °C, molten $V_2O_5$ first reacts with $Gd_2Zr_2O_7$ to form

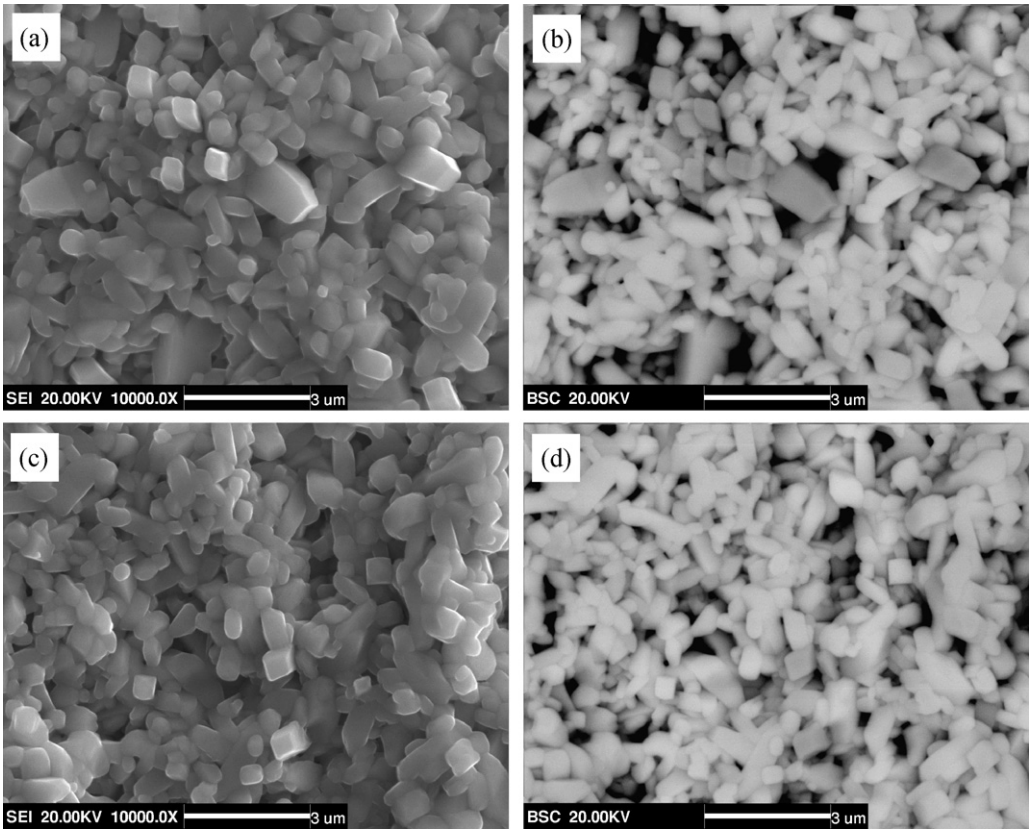


Fig. 6. Microstructures of $V_2O_5$-coated $Gd_2Zr_2O_7$ specimens heat-treated at 800 and 850 °C for 2 h: (a and c) secondary electron micrographs after heat-treatments at 800 and 850 °C for 2 h, respectively; (b and d) corresponding backscattered electron micrographs of (a) and (c), respectively.

$ZrV_2O_7$ and $GdVO_4$. The reaction mechanism at 700 °C is given by the following chemical equation:

$$3V_2O_5(l) + Gd_2Zr_2O_7(s) \rightarrow 2ZrV_2O_7(s) + 2GdVO_4(s) \quad (1)$$

According to the phase diagram in the $ZrO_2$–$V_2O_5$ binary system, $ZrV_2O_7$ was the only existent compound in this system.[19] At about 747 °C, $ZrV_2O_7$ melts incongruently to m-$ZrO_2$ and a liquid mixture of m-$ZrO_2$ and $V_2O_5$.[19,20] This incongruent melting results in different chemical reactions observed at temperatures of 700 °C and 750–850 °C, respectively. Above 747 °C, i.e., 750–850 °C in this study, molten $V_2O_5$ from the incongruent melting of $ZrV_2O_7$ reacts with $Gd_2Zr_2O_7$ to form $ZrV_2O_7$ and $GdVO_4$, as shown in Eq. (1). At the same time, $ZrV_2O_7$ melts incongruently to m-$ZrO_2$ and a liquid mixture of m-$ZrO_2$ and $V_2O_5$. Finally, $V_2O_5$ is depleted, and the final reaction products are $GdVO_4$ and m-$ZrO_2$. The reaction mechanism at temperatures of 750–850 °C is given by the following chemical equation:

$$V_2O_5(l) + Gd_2Zr_2O_7(s) \rightarrow 2GdVO_4(s) + 2m\text{-}ZrO_2(s) \quad (2)$$

## 4. Conclusions

Molten $V_2O_5$ reacted with $Gd_2Zr_2O_7$ ceramic prepared by pressureless-sintering in the temperature range of 700–850 °C. At 700 °C, molten $V_2O_5$ reacted with $Gd_2Zr_2O_7$ to form $ZrV_2O_7$ and $GdVO_4$. However, in a temperature range of 750–850 °C, molten $V_2O_5$ reacted with $Gd_2Zr_2O_7$ to form $GdVO_4$ and m-$ZrO_2$. The two different reactions observed at 700 °C and 750–850 °C could be explained based on the thermal instability of $ZrV_2O_7$.

## Acknowledgements

The authors would like to thank the financial support from the Program of Excellent Teams in Harbin Institute of Technology (HIT) and the Start-up Program for High-level HIT Faculty Returned from Abroad.

## References

1. Padture, N. P., Gell, M. and Jordan, E. H., Thermal barrier coatings for gas-turbine engine applications. *Science*, 2002, **296**, 280–284.
2. Vaßen, R., Cernuschi, F., Rizzi, G., Scrivani, A., Markocsan, N., Östergren, L. *et al.*, Recent activities in the field of thermal barrier coatings including burner rig testing in the European union. *Adv. Eng. Mater.*, 2008, **10**, 907–921.
3. Evans, A. G., Clarke, D. R. and Levi, C. G., The influence of oxides on the performance of advanced gas turbines. *J. Eur. Ceram. Soc.*, 2008, **28**, 1405–1419.
4. Kisi, E. H. and Howard, C. J., Crystal structures of zirconia phases and their inter-relation. *Key Eng. Mater.*, 1998, **153–154**, 1–36.
5. Cao, X. Q., Vassen, R. and Stőver, D., Ceramic materials for thermal barrier coatings. *J. Eur. Ceram. Soc.*, 2004, **24**, 1–10.
6. Andrievskaya, E. R., Phase equilibria in the refractory oxide systems of zirconia, hafnia and yttria with rare-earth oxides. *J. Eur. Ceram. Soc.*, 2008, **28**, 2363–2388.
7. Suresh, G., Seenivasan, G., Krishnaiah, M. V. and Murti, P. S., Investigation of the thermal conductivity of selected compounds of lanthanum, samarium and europium. *J. Alloys Compd.*, 1998, **269**, L9–L12.
8. Vassen, R., Cao, X., Tietz, F., Basu, D. and Stőver, D., Zirconates as new materials for thermal barrier coatings. *J. Am. Ceram. Soc.*, 2000, **83**, 2023–2028.
9. Wu, J., Wei, X. Z., Padture, N. P., Klemens, P. G., Gell, M., Garcia, E. *et al.*, Low-thermal-conductivity rare-earth zirconates for potential thermal-barrier-coating applications. *J. Am. Ceram. Soc.*, 2002, **85**, 3031–3035.
10. Lehmann, H., Pitzer, D., Pracht, G., Vassen, R. and Stőver, D., Thermal conductivity and thermal expansion coefficients of the lanthanum rare-earth-element zirconate system. *J. Am. Ceram. Soc.*, 2003, **86**, 1338–1344.
11. Liu, Z.-G., Ouyang, J.-H., Zhou, Y., Li, J. and Xia, X.-L., Influence of ytterbium- and samarium-oxides codoping on structure and thermal conductivity of zirconate ceramics. *J. Eur. Ceram. Soc.*, 2009, **29**, 647–652.
12. Michel, D., Perez-y-Jorba, M. and Collongues, R., Etude de la transformation ordre–desordre de la structure fluorite a la structure pyrochlore pour des phases $(1-x)ZrO_2$–$xLn_2O_3$. *Mater. Res. Bull.*, 1974, **9**, 1457–1468.
13. Bose, S., *High temperature coatings*. Elsevier Inc., Burlington, 2007, pp. 55–70.
14. Jones, R. L., Some aspects of the hot corrosion of thermal barrier coatings. *J. Therm. Spray Technol.*, 1997, **6**, 77–84.
15. Mohan, P., Yuan, B., Patterson, T., Desai, V. H. and Sohnw, Y. H., Degradation of yttria-stabilized zirconia thermal barrier coatings by vanadium pentoxide, phosphorous pentoxide, and sodium sulfate. *J. Am. Ceram. Soc.*, 2007, **90**, 3601–3607.
16. Chen, Z., Speakman, S., Howe, J., Wang, H., Porter, W. and Trice, R., Investigation of reactions between vanadium oxide and plasma-sprayed yttria-stabilized zirconia coatings. *J. Eur. Ceram. Soc.*, 2009, **29**, 1403–1411.
17. Chen, Z., Mabon, J., Wen, J.-G. and Trice, R., Degradation of plasma-sprayed yttria-stabilized zirconia coatings via ingress of vanadium oxide. *J. Eur. Ceram. Soc.*, 2009, **29**, 1647–1656.
18. Marple, B. R., Voyer, J., Thibodeau, M., Nagy, D. R. and Vassen, R., Hot corrosion of lanthanum zirconate and partially stabilized zirconia thermal barrier coatings. *J. Eng. Gas Turb. Power*, 2006, **128**, 144–152.
19. Reser, M. K., ed., *Phase diagrams for ceramists—1969 supplement, Fig. 2405*. American Ceramic Society, Columbus, OH, 1969.
20. Buchanan, R. C. and Wolter, G. W., Properties of hot-pressed zirconium pyrovanadate ceramics. *J. Electrochem. Soc.*, 1983, **130**, 1905–1910.